Journal of Magnetic Resonance **144,** 162–167 (2000)
doi:10.1006/jmre.2000.2037, available online at http://www.idealibrary.com on IDEAL®

Imaging Membrane Protein Helical Wheels

J. Wang,* J. Denny,† C. Tian,* S. Kim,* Y. Mo,‡ F. Kovacs,* Z. Song,§ K. Nishimura,§ Z. Gan,§ R. Fu,§ J. R. Quine,†,§ and T. A. Cross,*,‡,§

§*National High Magnetic Field Laboratory, *Institute of Molecular Biophysics, †Department of Mathematics, and ‡Department of Chemistry, Florida State University, Tallahassee, Florida 32310*

Received September 2, 1999; revised January 25, 2000

Resonance patterns have been observed in 2D solid-state NMR spectra of the transmembrane segment of M2 protein from Influenza A virus in oriented samples reflecting the helical wheel of this α-helix. The center of this pattern uniquely defines the helical tilt with respect to the bilayer normal without a need for resonance assignments. The distribution of resonances from amino acid specific labels around the "PISA wheel" defines the rotational orientation of the helix and yields preliminary site-specific assignments. With assignments high-resolution structural detail, such as differences in tilt and rotational orientation along the helical axis leading to an assessment of helical coiling, can be obtained. © 2000 Academic Press

Key Words: **PISEMA; ^{15}N solid-state NMR; orientational constraints; membrane proteins; oriented samples.**

INTRODUCTION

Macromolecular structure determination by NMR spectroscopy has been absolutely dependent on resonance assignments. Indeed, inaccurate assignments have frequently led to incorrect structures. Achieving the set of accurate resonance assignments for a structural characterization is a very substantial task in solution NMR and a daunting task in solid-state NMR where methods are just now being developed (*1, 2*). Here we demonstrate that resonance patterns from membrane protein helices are present in solid-state NMR spectra representing helical wheels and obviating the need for assignments prior to achieving an initial structural characterization.

Solid-state NMR-derived orientational constraints from samples with one-, two-, or three-dimensional order can be used to solve high-resolution structure from a lamellar phase lipid environment (*3–5*). PISEMA (polarization inversion spin exchange at the magic angle) is a major improvement over previous experiments that correlate anisotropic dipolar and chemical shift interactions (*6*). The use of a frequency-switched Lee–Goldburg pulse sequence to perform ^{1}H homonuclear decoupling has resulted in far better resolution in the dipolar dimension. Two spectra displaying tens to hundreds of resonances have been recorded (*7*) of uniformly ^{15}N-labeled proteins setting the stage for structure determination. Previously, it has been noted that resonances having near maximal dipolar splitting at the low field edge of the chemical shift range (σ_{33}) suggest transmembrane helices, since the N–H bonds in α-helices are nearly parallel to the helix axis (*8, 9*). Likewise resonances at the high field edge of the chemical shift range (σ_{11}) that have a half-maximal dipolar splitting suggest helices that are parallel to the bilayer surface. Here we recognize that α-helices give rise to unique resonance patterns in these spectra and that the center of the pattern uniquely reflects the specific tilt angle of the helical axis with respect to the bilayer normal. The rotational orientation about the helical axis can also be determined. In a parallel and complementary study Marassi and Opella have independently observed the same phenomena in the PISEMA spectra of membrane polypeptides and present their results in the accompanying paper (*10*).

The unique qualities of such observations are exemplified with spectra of the transmembrane peptide of the Influenza A viral M2 protein. M2 protein, which forms a H^{+} channel in the viral coat, provides an essential function during the viral life cycle (*11, 12*). This protein possesses a single transmembrane helix (residues 25–43) and as a tetramer it forms a channel that is pH gated (*13, 14*). A peptide (M2-TMP, residues 22–46) has also been shown to conduct protons and to be blocked by the antiviral drug, amantadine (*15, 16*).

RESULTS

In Fig. 1 slices through the dipolar dimension of ^{15}N PISEMA spectra from several single and multiple site labeled samples of M2-TMP are combined. These sites are assigned by virtue of single site labeled preparations achieved by solid phase peptide synthesis (*17*; Song *et al.,* unpublished results). By connecting the resonances within each dipolar transition, a mirror image pair of "PISA wheels" (polarity index slant angle) is immediately apparent.

Simulations of this phenomenon are displayed in Fig. 2B by calculating the ^{15}N anisotropic chemical shift and ^{15}N–^{1}H dipolar interactions for different helical tilts, τ. Since the repeat unit of an ideal α-helical structure ($\phi = -65°$, and $\psi = -40°$) is a single peptide plane, these patterns can be calculated by simply rotating the helix about its axis by ρ, while calculating the dipolar and chemical shift observables. The PISA wheels result from the noncollinearity of the chemical shift and dipolar

1090-7807/00 $35.00

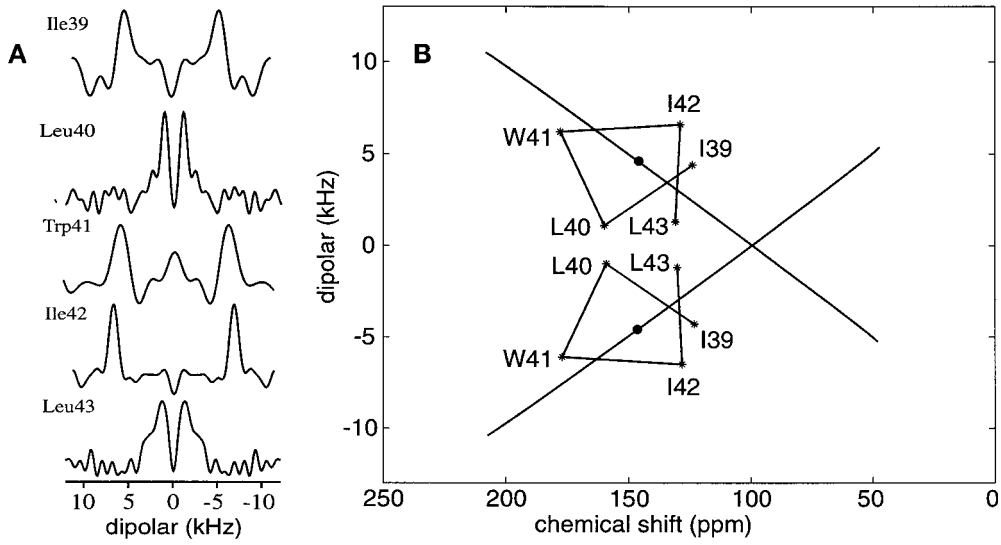

FIG. 1. (A) Dipolar splittings observed from PISEMA spectra of multiple and single site labeled preparations of M2-TMP in hydrated lipid bilayers aligned with the bilayer normal parallel to the magnetic field direction. The spectra were obtained (Song *et al.*, unpublished results) with a 400-MHz spectrometer using a Chemagnetics data acquisition system and a 9.4-T wide-bore Oxford Instruments magnet. An RF field strength of 38.5 kHz was used for the Lee–Goldburg (LG) condition corresponding to a LG time increment of 26 μs. A delay of 1 μs was given at the onset of each $\pm$LG cycle to compensate for the frequency synthesizer (PTS) switch time. The t_1 duration was incremented from 0 to 24 LG cycles and the refocused ^{15}N signal was typically acquired with 2000 transients for each t_1 increment. Spectral symmetry in the dipolar dimension was achieved by setting the imaginary part of the data to zero before the Fourier transform against t_1. The experimental error in the chemical shift dimension is $\pm$5 ppm and in the dipolar dimension it is $\pm$1 kHz. (B) Display of the dipolar splittings (*) at their observed chemical shift. The resonances are connected in helical wheel fashion. Since the two wheels are mirror images displaying identical information, only one will be used in the following figures.

interaction tensors and the fact that the near-unique tensor elements are not aligned parallel to the helical axis. The following equations are developed using an ideal helix, standard bond angles for peptide planes, and standard values for the relative orientation of the dipolar and chemical shift tensors.

$$\begin{aligned}\mathbf{F}(\rho, \tau) &= (\text{chemical shift}(\rho, \tau), \text{dipolar splitting}(\rho, \tau))\\ &= (\sigma_{11}(-0.828\cos\rho\sin\tau + 0.558\sin\rho\sin\tau\\ &\quad - 0.047\cos\tau)^2 + \sigma_{22}(0.554\cos\rho\sin\tau\\ &\quad + 0.803\sin\rho\sin\tau - 0.220\cos\tau)^2\\ &\quad + \sigma_{33}(-0.088\cos\rho\sin\tau - 0.206\sin\rho\sin\tau\\ &\quad - 0.975\cos\tau)^2, \frac{\nu_\parallel}{2}(3(-0.326\cos\rho\sin\tau\\ &\quad - 0.034\sin\rho\sin\tau - 0.946\cos\tau)^2 - 1))\end{aligned} \quad [1]$$

For a tilted helix, the plot of the PISA wheels is generated by graphing the set

$$S(\tau) = \{\mathbf{F}(\rho, \tau): \rho \in [0, 2\pi)\}. \quad [2]$$

To examine the behavior of **F** as the helix tilt increases, we define the *center* of $S(\tau)$ to be the average value of **F** over the interval

$$\begin{aligned}\text{Avg}(\tau) &= \frac{1}{2\pi}\int_0^{2\pi}\mathbf{F}(\rho, \tau)d\rho\\ &= (0.950\sigma_{33}\cos^2\tau + (0.500\sigma_{11}\\ &\quad + 0.476\sigma_{22})\sin^2\tau, 0.081\nu_\parallel\sin^2\tau\\ &\quad + 1.34\nu_\parallel\cos^2\tau - 0.500\nu_\parallel).\end{aligned} \quad [3]$$

This integral has the same effect as averaging the CSA and dipolar tensors about the helix axis.

In an experimental PISEMA spectrum, the wheel is composed of a set of discrete resonances—one of each peptide plane. The center of the PISA wheel is uniquely governed by helix tilt and, as a function of tilt angle, forms an "X" pattern characteristic of collinear tensors (*18*). Here the tensors become collinear because of the "tensorial averaging" or rotation about the helix axis done just for this calculation. The experimental data is not on the X because the unique tensor elements are not collinear with the helix axis.

In Fig. 2C, a more extensive collection of data from M2-TMP is represented and overlaid with calculated PISA wheels having tilt angles of 35, 38, and 41°. In this way the tilt angle is shown to be 38 $\pm$ 3°, consistent with the tilt angle calculated from a set of assigned chemical shifts and from this set of assigned PISEMA results (*17*; Song *et al.*, unpublished results). However, the conclusion here is achieved without any use or need for resonance assignments.

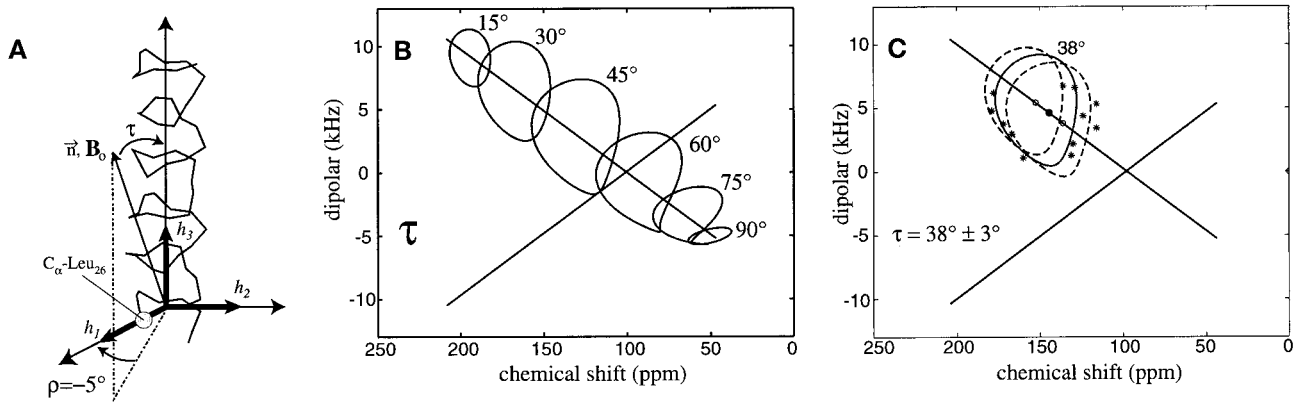

FIG. 2. The origins of the "PISA wheels." For the analysis in this manuscript, n, the bilayer normal, is always aligned parallel to B_0. (A) Definitions of τ and ρ for an α-helix. $\tau = 0°$ occurs when the helix axis, h_3, is parallel to B_0. $\rho = 0°$ occurs when the projection of B_0 onto a plane perpendicular to h_3 makes an angle of 0° with h_1, the radial axis of the helix that passes through the C_α carbon of Leu_{26}. (B) "Circles" drawn for one of the dipolar transitions using average values of tensor elements ($\tau_{11} = 31.3$, $\tau_{22} = 55.2$, $\sigma_{33} = 201.8$ ppm) and the relative orientations of the dipolar and chemical shift tensor, given by $\theta = 17°$, the angle in the peptide plane between σ_{33} and $\nu_\parallel$ (parallel to the N–H bond). The circles for the other dipolar transitions are the mirror image about 0 kHz. (C) Characterization of the M2-TMP helix tilt from a more complete set of PISEMA data than that presented in Fig. 1. The data are consistent with a helix tilt of 38 ± 3°. Note that the center of the PISA wheels falls on a line that passes through the isotropic chemical shift (96 ppm) at 0 kHz on the dipolar scale.

Moreover, the rotational orientation of the helix, ρ, can be determined from amino acid specific labeling. By choosing an amino acid with an asymmetric distribution about the helical wheel, the asymmetric distribution will be reflected in the PISA wheel. A PISEMA spectrum of ^{15}N $Ile_{32,33,35,39,42}$-labeled M2-TMP shows (Fig. 3A) the high resolution of this experiment. Here four of the resonances are within a 100° arc on the helical wheel, as shown on the horizontal scale of Fig. 3C, while the fifth isoleucine resonance is separated from the others by 100°. The PISEMA data are analyzed by using the previously determined PISA wheel (Fig. 2C) with a helical tilt of 38°. The pattern is dissected into angular domains for assessing an experimental ρ value for each resonance (Fig. 3B). These values are plotted against the predicted ρ values assuming an ideal helix of 3.60 residues per turn. The linear extrapolation with a slope of 1.0 characterizes the y intercept, $\rho_0(27–43) = -5 \pm 10°$. Once again such an analysis is not dependent on resonance assignments, but can be achieved using a best fit approach of the experimental and predicted ρ values. However, it is also possible to view this process as a preliminary assignment method. The determination of ρ_0 is consistent with previous determinations (*17*, *19*).

Figure 4A displays the experimental data along with the best fit defined from the analysis in Fig. 3. The best fit leads to a complete predicted helical wheel (Fig. 4B). Such a wheel can be compared to the independently assigned data displayed in

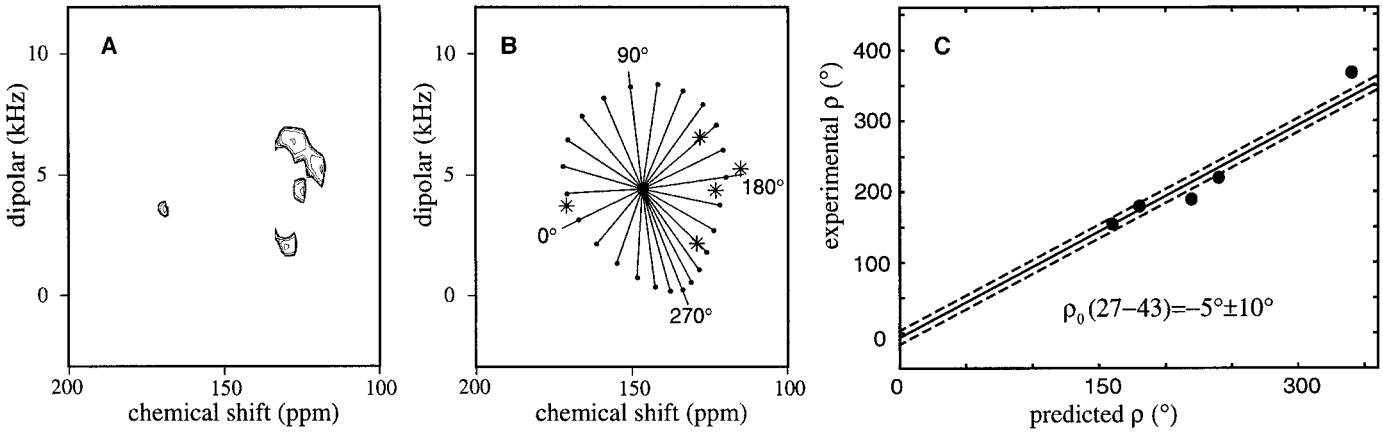

FIG. 3. (A) The ^{15}N $Ile_{32,33,35,39,42}$-labeled M2-TMP PISEMA spectrum obtained as in Fig. 1. Most of the resonances have been assigned based on single-site isotopic labels, but here the analysis has no dependence on such assignments. (B) Based on Eq. [1], the "PISA wheels" can be dissected into domains of ρ angles for cataloging an experimental value of ρ for each resonance. (C) The experimental ρ values are compared to predicted values based on residue number and 100°/residue for an ideal helix. Predicted and experimental values are paired by solving for a best fit. The result is an extrapolation and intersection with the experimental axis at $\rho_0 = -5 \pm 10°$.

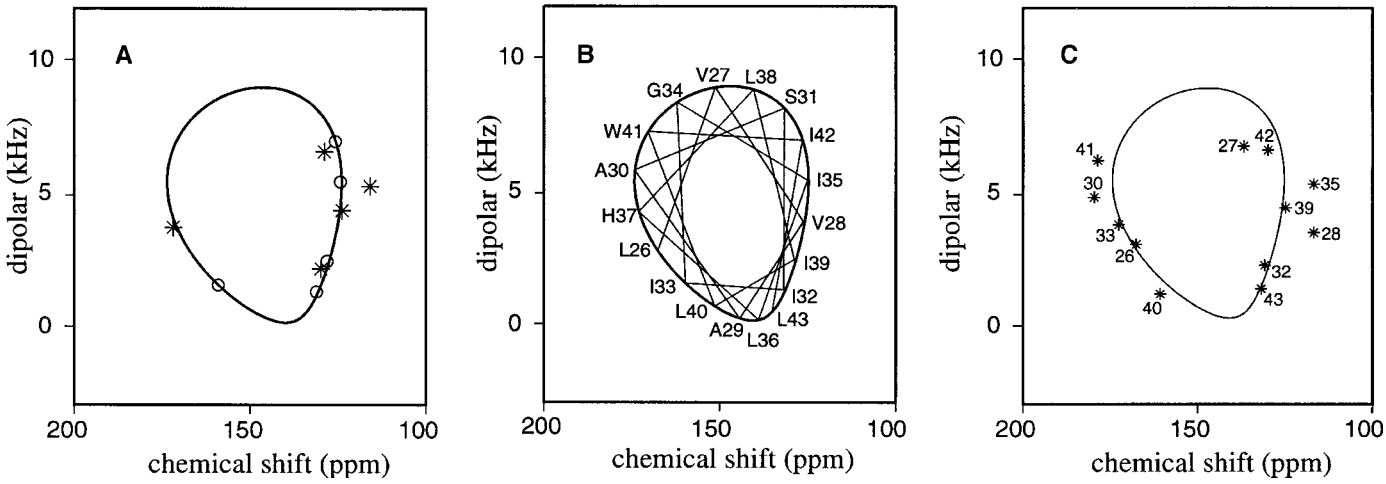

FIG. 4. (A) Best fit (○) to the 5-site Ile-labeled M2-TMP PISEMA resonances (*) based on the analysis in Fig. 3. (B) From this analysis and the resulting assignment of resonances, the helical wheel for this hydrophobic transmembrane peptide can be predicted. (C) The predicted resonance positions from the helical wheel are compared to the experimental data.

Fig. 4C. For many reasons the experimental data do not deliver an ideal helical wheel. Variation in τ and ρ along the length of the helix could generate scatter in the experimental data; however, based on the data set in Fig. 4C there appears to be little evidence for nonuniform values of τ and ρ along the length of the helix.

While changes in ρ and τ along the length of the helix are a potential source of imperfections for these PISA wheels, there are others. Differences in the chemical shift tensor (Table 1) result in perturbations, as shown in Fig. 5A, that may account for much of the scatter in the experimental data. The relative orientation of the ^{15}N chemical shift and ^{15}N–^{1}N dipolar interaction tensors also influences the PISA wheel (Fig. 5B). In particular, the shape of the pattern is extended in a direction that is nearly perpendicular to the line formed by the pattern's center as a function of helix tilt. The best fit value of 17° corresponds to a β_D angle of 105°. This value of β_D represents a typical chemical shift tensor orientation for nonglycine amides (*20–24*). From this figure it is clear that the experimental data are consistent with little variation in θ. This may be the result of more uniform secondary structure in a membrane environment than in an aqueous environment where a greater variation in θ for α-helices has recently been suggested (*25*).

Another potential source for scatter in the experimental data is local distortion of the helix. Compensated changes in torsion angles can tilt the peptide planes without significantly altering the number of residues per turn or the pitch of the helix. Such distortions are typically induced by proline and glycine, but other circumstances may cause variation in the tilt of the peptide planes relative to the helix axis, δ. In Fig. 5C such variations are illustrated and demonstrate that the influence of δ on the PISA wheels is essentially parallel to the line formed by the centers of the patterns as a function of helix tilt. Consequently, the influence of δ is essentially orthogonal to that of θ, making the characterizations of θ and δ essentially independent. Once again, it is clear that the experimental data are consistent with little variation in δ.

DISCUSSION

The observation of helical wheels in the PISEMA spectra provides a mechanism to obtain detailed structural information without resonance assignments. Prior to this observation, resonance assignments have been a prerequisite for significant structural conclusions. Not only are the global tilt and rotational orientation determinable from PISEMA data, but the clear observation of a PISA wheel places very substantial limits on the variation of helix tilt from one end of the helix to the other and on local distortions within the helix. These PISA wheels can be observed, not only in the PISEMA spectra of M2-TMP, but also in the M2δ peptide from acetylcholine receptor (*5, 10*), in the colicin E1 channel domain (*26*), and in the fd coat protein (*27*) as well. These spectra have all been obtained from samples solubilized in lamellar phase phospholipid bilayers, and even the presence of PISA wheels suggests that transmembrane α-helices have few distortions, such as kinks and bends, and that they have near ideal and uniform local structure.

Many membrane proteins have numerous transmembrane helices, which will compromise the observation of discrete PISA wheels in uniformly ^{15}N-labeled samples. However, frequently membrane proteins can be cleaved at the loops between helices with little loss of functional activity. This may provide an opportunity to label individual helices or pairs of helices while the remainder is unlabeled. The recent demonstration of segmental labeling using inteins also provides a potential mechanism for simplifying PISEMA spectra of uniformly labeled proteins (*25*).

Alternative and laborious methods have been described for achieving less structural information for a variety of systems.

TABLE 1
Chemical Shift Tensor Element Magnitudes for the Observed Sites in M2-TMP[a]

Site	σ_{11}	σ_{22}	σ_{33}
Val27	33	55	198
Val28	29	53	202
Ile32	35	59	208
Ile33	31	54	202
Ile35	32	56	210
Ile39	30	54	195
Leu40	32	55	203
Trp41	32	56	205
Ile42	30	54	198
Leu43	29	56	200

[a] The chemical shift anisotropy has been determined from single site labeled samples of M2-TMP. Spectra were obtained of samples dried from trifluoroethanol where the peptide is observed to be α-helical; it is likely, therefore, that the peptides for this characterization are in the conformation of interest.

The use of single site labels previously led to a determination of global τ and ρ_0 in M2-TMP (*17*) and indirectly for the assignment of a uniformly labeled helix, M2δ of the acetylcholine receptor for the characterization of τ (*5*). Infrared spectroscopy of oriented, single-site isotopically labeled M2-TMP has also been used to determine τ and ρ_0 (*19*). Electron spin resonance methods have also used single site labels arranged on helices through single-site cysteine mutagenesis to determine helix tilts and rotational orientations (*28, 29*). For the solid-state NMR approach, the incorporation of bulky and potentially perturbing spin labels is not necessary. Now spectra of uniformly labeled proteins, even in the absence of assignments, can give rise to substantial structural conclusions. This is possible through the unique pattern of resonances in PISEMA spectra that directly reflect the protein structure.

While several aspects and implications of the PISA wheels have been described here the potential for future development is great. For instance, changes in ρ along the length of a helix will reflect coiling of the helix in a helical bundle. Additionally, the aqueous exposure of the M2 four-helix bundle along the bundle axis should result in rapid exchange of amide protons for deuterons along this channel axis eliminating resonances from just a segment of the PISA wheel, immediately identifying the portion of the helix exposed to the channel. Not only can transmembrane helices be characterized, but also those on the surface of the bilayer will give rise to PISA wheels as well. However, for these wheels a mirror plane exists parallel to the plane of the bilayer, resulting in a full turn of the PISA wheel in just 180° of the helical wheel. H/D exchange for these helices will not yield as simple an image as for the transmembrane helices. Such surface associated helices will also be sensitive to variations in α_D, the angle of the N–C_1 bond projection in the σ_{22}/σ_{11} plane to the σ_{11} axis. The transmembrane PISA wheels are not sensitive to this parameter and to the relative magnitude of σ_{11} and σ_{22}, but the helices parallel to the bilayer surface will be sensitive to these factors. Clearly, the PISEMA experiment opens new and exciting avenues for research into the structure of membrane proteins.

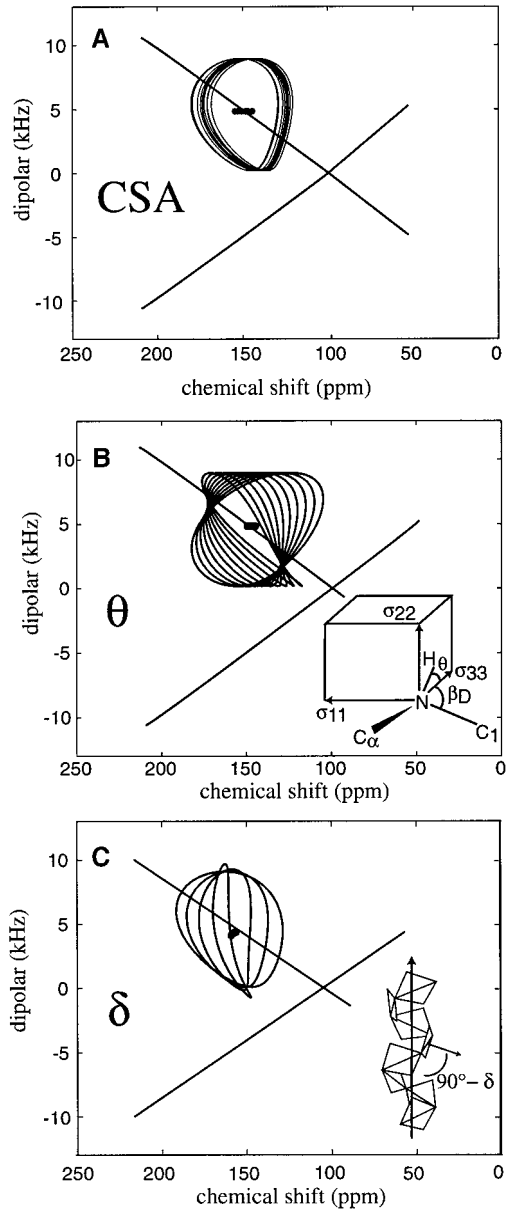

FIG. 5. The chemical shift anisotropy (CSA), relative orientation of chemical shift and dipolar tensors (θ), and local variation in helical structure through compensated peptide plane tilts (δ) are potential sources of distortion for the PISA wheel. (A) The chemical shift anisotropy has been determined from single site labeled samples of M2-TMP. The calculation of a "PISA wheel" using each of these CSA tensors (Table 1) is displayed showing significant variation in both the pattern and the calculation of its center. (B) The influence of θ on the PISA wheel is dramatic, but shows little effect on the pattern's center. The range of θ values displayed is 5 to 23° in 2° increments, where $\theta + \beta_D = 122°$, the HNC_1 bond angle. The value $\theta = 17°$ corresponding to $\beta_D = 105°$ has been used in all other figures. (C) The influence of peptide plane tilt on the shape of the PISA wheel is also dramatic, but there is little effect on the center of the pattern. The δ values displayed are 0, 5, 8.7, and 12°. The ideal helix has peptide plane tilts of $\delta = 8.7°$, the value used in all other figures.

ACKNOWLEDGMENTS

The authors are indebted to S. J. Opella and F. M. Marassi for sharing their manuscript with us prior to submission. The authors also thank the staff of the NHMFL NMR facility, in particular, A. Blue, as well as the staff of the Bioanalytical Synthesis and Services Laboratory, H. Henricks and U. Goli, for their expertise and maintenance of the instrumentation essential for this effort. This work was supported by the National Science Foundation, DMB 9603935 (T.A.C. and J.R.Q.) and DBI 9602233 (J.K.D.). The work was largely performed at the National High Magnetic Field Laboratory supported by NSF Cooperative Agreement (DMR-9527035) and the State of Florida.

REFERENCES

1. M. Hong and R. G. Griffin, Resonance assignments for solid peptides by dipolar-mediated $^{13}C/^{15}N$ correlation solid-state NMR, *J. Am. Chem. Soc.* **120,** 7113–7114 (1998).
2. F. M. Marassi, J. J. Gesell, A. P. Valente, Y. Kim, M. Oblatt-Montal, M. Montal, and S. J. Opella, Dilute spin-exchange assignment of solid-state NMR spectra of oriented proteins: acetylcholine M2 in bilayers, *J. Biomol. NMR* **14,** 141–148 (1999).
3. R. R. Ketchem, W. Hu, and T. A. Cross, High resolution conformation of gramicidin A in a lipid bilayer by solid-state NMR, *Science* **261,** 1457–1460 (1993).
4. R. R. Ketchem, B. Roux, and T. A. Cross, High-resolution polypeptide structure in a lamellar phase lipid environment from solid-state NMR derived orientational constraints, *Structure* **5,** 1655–1669 (1997).
5. S. J. Opella, F. M. Marassi, J. J. Gesell, A. P. Valente, Y. Kim, M. Oblatt-Montal, and M. Montal, Structures of the M2 channel-lining segments from nicotinic acetylcholine and NMDA receptors by NMR spectroscopy, *Nat. Struct. Biol.* **6,** 374–379 (1999).
6. C. H. Wu, A. Ramamoorthy, and S. J. Opella, High-resolution heteronuclear dipolar solid-state NMR spectroscopy, *J. Magn. Reson. A* **109,** 270–274 (1994).
7. F. M. Marassi and S. J. Opella, NMR structural studies of membrane proteins, *Curr. Opin. Struct. Biol.* **8,** 640–648 (1998).
8. K.-J. Shon, Y. Kim, L. A. Colnago, and S. J. Opella, NMR studies of the structure and dynamics of membrane-bound bacteriophage Pf1 coat protein, *Science* **252,** 1303–1305 (1991).
9. T. A. Cross and S. J. Opella, Solid state NMR structural studies of peptides and proteins in membranes, *Curr. Opin. Struct. Biol.* **4,** 574–581 (1994).
10. F. M. Marassi and S. J. Opella, A solid-state NMR index of helical membrane proteins structure and topology, *J. Magn. Reson.* **144,** 150–155 (2000).
11. A. J. Hay, The action of adamantamines against Influenza A virus: Inhibition of the M2 ion channel protein, *Semin. Virol.* **3,** 21–30 (1992).
12. R. A. Lamb and R. M. Krug, Orthomyxoviridae: The viruses and their replication, *in* "Field's virology" (B. N. Fields, D. M. Knipe, and P. M. Howley, Eds.), p. 1353. Lippincot–Raven, Philadelphia (1996).
13. T. Sakaguchi, Q. Tu, L. H. Pinto, and R. A. Lamb, The active oligomeric state of the minimalistic Influenza virus M2 ion channel is a tetramer, *Proc. Natl. Acad. Sci. USA* **94,** 5000–5005 (1997).
14. D. Salom, J. D. Lear, and W. F. DeGrado, Aggregation of Influenza A M2 transmembrane segment in micelles, *Biophys. J.* **76,** A123 (1999).
15. K. C. Duff and R. H. Ashley, The transmembrane domain in Influenza A M2 protein forms amantadine-sensitive proton channels in planar lipid bilayers, *Virology* **190,** 485–489 (1992).
16. K. C. Duff, S. M. Kelly, N. C. Price, and J. P. Bradshaw, The secondary structure of Influenza A M2 transmembrane domain. A circular dichroism study, *FEBS Lett.* **311,** 256–258 (1992).
17. F. A. Kovacs and T. A. Cross, Transmembrane four-helix bundle of Influenza A M2 protein channel: Structural implications from helix tilt and orientation, *Biophys. J.* **73,** 2511–2517 (1997).
18. F. Tian, Z. Song, and T. A. Cross, Orientational constraints derived from hydrated powder samples by two-dimensional PISEMA, *J. Magn. Reson.* **135,** 227–231 (1998).
19. A. Kukol, P. D. Adams, L. M. Rice, A. T. Brunger, and I. T. Arkin, Experimentally based orientational refinement of membrane protein models: A structure for the Influenza A M2 H^+ channel, *J. Mol. Biol.* **286,** 951–962 (1999).
20. G. S. Harbison, L. W. Jelinski, R. E. Stark, D. A. Torchia, J. Herzfeld, and R. G. Griffin, ^{15}N Chemical shift and $^{15}N–^{13}C$ dipolar tensors for the peptide bond in [1-^{13}C]glycyl[^{15}N]glycine hydrochloride monohydrate, *J. Magn. Reson.* **60,** 79–82 (1984).
21. C. J. Hartzell, M. Whitfield, T. G. Oas, and G. P. Drobny, Determination of the ^{15}N and ^{13}C chemical shift tensors of L-[^{13}C]alanyl-L-[^{15}N]alanine from the dipole-coupled powder patterns, *J. Am. Chem. Soc.* **109,** 5966–5969 (1987).
22. T. G. Oas, C. J. Hartzell, F. W. Dahlquist, and G. P. Drobny, The amide ^{15}N chemical shift tensors of four peptides determined from ^{13}C dipole-coupled chemical shift powder patterns, *J. Am. Chem. Soc.* **109,** 5962–5966 (1987).
23. Q. Teng and T. A. Cross, The *in situ* determination of the ^{15}N chemical shift tensor orientation in a polypeptide, *J. Magn. Reson.* **85,** 439–447 (1989).
24. W. Mai, W. Hu, C. Wang, and T. A. Cross, Three dimensional structural constraints in the form of orientational constraints from chemical shift anisotropy: The polypeptide backbone of gramicidin A in a lipid bilayer, *Prot. Sci.* **2,** 532–542 (1993).
25. D. Fushman, N. Tjandra, and D. Cowburn, Direct measurement of ^{15}N chemical shift anisotropy in solution, *J. Am. Chem. Soc.* **120,** 10947–10952 (1998).
26. Y. Kim, K. Valente, S. J. Opella, S. L. Schendel, and W. A. Cramer, Solid-state NMR studies of the membrane-bound closed state of the colicin E1 channel domain in lipid bilayers, *Prot. Sci.* **7,** 342–348 (1998).
27. F. Marassi, A. Ramamoorthy, and S. J. Opella, Complete resolution of the solid-state NMR spectrum of a uniform ^{15}N-labeled membrane protein in phospholipid bilayers, *Proc. Natl. Acad. Sci. USA* **94,** 8551–8556 (1997).
28. D. L. Farrens, C. Altenbach, K. Yang, W. L. Hubble, and H. G. Khorana, Requirement of rigid-body motion of transmembrane helices for light activation of Rhodopsin, *Science* **274,** 768–770 (1996).
29. E. Perozo, D. M. Cortes, and L. G. Cuello, Structural rearrangements underlying K^+-channel activating gating, *Science* **285,** 73–78 (1999).